Songklanakarin J. Sci. Technol.
37 (3), 327-343, May-Jun. 2015

http://www.sjst.psu.ac.th

Original Article

Ab initio computational study of vincristine as a biological active compound: NMR and NBO analyses

Shiva Joohari* and Majid Monajjemi

Department of Chemistry, Science and Research Branch, Islamic Azad University, Tehran, 147893855 Iran.

Received: 15 October 2014; Accepted: 9 April 2015

Abstract

Vincristine is a biological active alkaloid that has been used clinically against a variety of neoplasms. In the current study we have theoretically investigated the magnetic properties of titled compound to predict physical and chemical properties of vincristine as a biological inhibitor. *Ab initio* computation using HF and B3LYP with 3-21G(d) and 6-31G(d) level of theory have been performed and then magnetic shielding tensor (σ, ppm), shielding asymmetry (μ), magnetic shielding anisotropy (σ_{aniso}, ppm), the skew of a tensor (K), chemical shift anisotropy (Δσ) and chemical shift (δ) were calculated to indicate the details of the interaction mechanism between microtubules and vincristine. Moreover, E_{HOMO}, E_{LUMO} and E_{bg} were evaluated. The maximum and minimum values of E_{bg} were found in HF/3-21g and B3LYP/3-21g respectively. It was also uggested that O_{24}, O_{37}, O_{49} and O_{55} with minimum values of σ_{iso}, are active sites of titled compound. Furthermore the calculated chemical shifts were compared with experimental data in DMSO and $CDCl_3$ solvents.

Keywords: vincristine, *ab initio*, NMR, NBO, biological, inhibitor.

1. Introduction

Vincristine is known as a powerful antitumor drug which has been applied for a long period of time in the treatment of various cancers and was originally discovered in the extracts of leaves of the Catharanthus rosea (Vinca rosea) plant (Noble *et al.*, 1958; Johnson *et al.*, 1959). Among the four extracted alkaloids, vincristine and vinblastine were known as biological active compounds (Johnson, 1968). Vincristine binds tubulin; thereby inhibiting the assembly of microtubules (Monajjemi *et al.*, 2010; Nafisi *et al.*, 2010; Martin-Galiano *et al.*, 2011; March *et al.*, 2011; Mollaamin *et al.*, 2014a). Molecular structure of vincristine has been presented in Scheme 1.

Scheme 1

In metaphase stage, microtubules are strongly bound to chromosomes placed in cell nucleus so that facilitates division of chromosomes. Vincristine can bind hardly to microtubules inhibiting from the division of chromosome and therefore stop cancer cell growth (Dowing and Nogals, 1998;

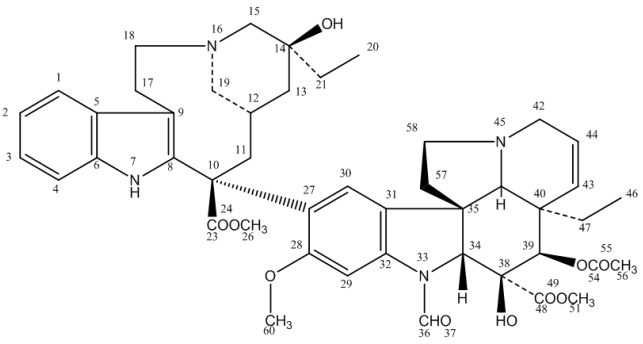

Scheme1. Molecular structure of vincristine.

* Corresponding author.
Email address: shjoohari@yahoo.com

Mordan, 2002; Jordan and Leslie, 2004; Lobert and Ingram, 2007; Gan and Kavallaris, 2008; Kavallaris *et al.*, 2008; Damen *et al.*, 2010; Kosjek *et al.*, 2013).

During the course of development of these alkaloids as chemotherapeutic agents, the unique observation was made that there is an exquisite sensitivity (Borman and Kuehne, 1990) in the structure-activity relationships concerning the stereochemistry at C-10, C-12, and C-14. In vinblastine and vincristine, the configuration at the C-10 stereogenic center is S while at C-12 it is *R* and at C-14 is S. The inversion of C-10 configuration from S to *R* results in a complete loss of activity as does C-12 conversion from *R* to S (Kuehne and Marko, 1990). The position at C-14 has also demonstrated to be especially critical concerning the interaction with tubulin (Borman and Kuehne, 1990; Dong *et al.*, 1995).

In continuation of previous studies (Monajjemi *et al.*, 2005; 2010; 2011a, 2011b; 2014a; Monajjemi and Boggs, 2013; Mollaamin *et al.*, 2014b), in this research we want to check the stability and chemical properties of vincristine by information obtained from computational methods and modeling.

2. Theoretical Background

The chemical shift refers to the phenomenon which associated with the secondary magnetic field created by the induced motions of the electrons that surrounding the nuclei when in the presence of an applied magnetic field. The energy of a magnetic momentum, μ, in a magnetic field, B, is as follow:

$$E = -\mu.(1-\sigma)B$$

where σ refers to the differential resonance shift due to the induced motion of the electrons. The chemical shielding is characterized by a real three-by-three Cartesian matrix, which can be divided into a single scalar term, three anti symmetric pseudo vector components, and five components corresponding to a symmetric tensor (Sefzic *et al.*, 2005). Only the single scalar and the five symmetric tensor elements can be seen in the normal NMR spectra of the solids. The chemical shift anisotropy (CSA) tensor can be explained by three additional parameters as following (Sefzic *et al.*, 2005; Mousavi *et al.*, 2013).

Accurate predictions of molecular response properties to external elds are important in various areas of chemical physics. This especially refers to the second-order magnetic response properties (NMR), since the magnetic resonance based on techniques have gained substantial importance in chemistry and biochemistry that NMR data shown with two parameters isotropic (σ_{iso}) and anisotropic (σ_{aniso}) shielding. If $|\sigma_{11}-\sigma_{iso}| \geq |\sigma_{33}-\sigma_{iso}|$, σ, chemical shift anisotropy, η, asymmetry parameter and δ are shown as below (Mousavi *et al.*, 2013):

$$\Delta\sigma = \sigma_{11} - \frac{\sigma_{22}+\sigma_{33}}{2}$$

$$\eta = \frac{\sigma_{22}-\sigma_{33}}{\delta}$$

$$\delta = \sigma_{11} - \sigma_{iso}$$

If $|\sigma_{11}-\sigma_{iso}| < \sigma_{33}-\sigma_{iso}|$:

$$\Delta\sigma = \sigma_{33} - \frac{\sigma_{22}+\sigma_{11}}{2}$$

$$\eta = \frac{\sigma_{22}-\sigma_{11}}{\delta}$$

$$\delta = \sigma_{33} - \sigma_{iso}$$

For both causes skew (K) is shown as:

$$K = \frac{3*(\sigma_{iso}-\sigma_{22})}{\sigma_{33}-\sigma_{11}}$$

The skew is a measure for the asymmetric probability distribution of a real-valued random variable about its mean. σ_{11}, σ_{22} and σ_{33} are diagonal elements of CSA tensor.

3. Computational Methods

Molecular structure of vincristine was optimized using HF and B_3LYP model with 3-21G(d) and 6-31G(d) basis set. Calculations were performed to study thermodynamic parameters extracted from NMR chemical shift data and NBO analysis (Monajjemi *et al.*, 2014b). All calculations were carried out using the Gaussian 09 program package. The optimized geometric structure of vincristine based on theoretical methods is shown in Figure 1.

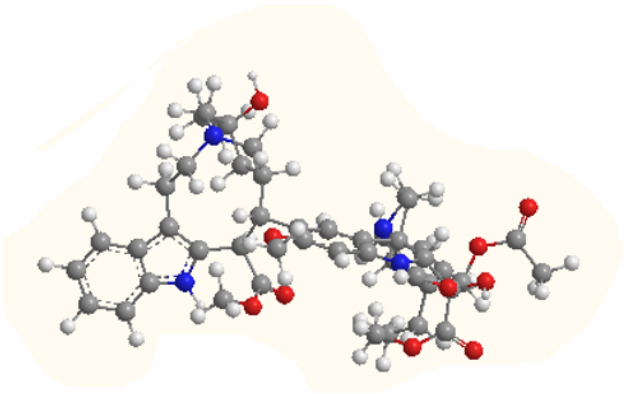

Figure 1. Optimized geometric structure of vincristine.

4. Results and Discussion

In this work we study magnetic properties of atomic nuclei to determine physical and chemical properties of atoms in the titled compound by NMR spectroscopy. Ab initio calculation of nuclear magnetic shielding has become an aid for the analysis of molecular structure. So, NMR is based on the quantum mechanical property of nuclei. Based on NMR study, calculated magnetic shielding tensor (σ, ppm), shielding asymmetry (η), magnetic shielding anisotropy (σ_{aniso}, ppm), the skew of a tensor (K), chemical shift anisotropy (Δσ) and chemical shift (δ) were calculated. These results are listed in Table 1 and 2. Graphs of these calculated parameters versus the number of atoms of vincristine were sketched as shown in Figure 2a-n, respectively.

As seen in Figure 2a-f and 3a-d, at HF model with 3-21G(d) basis set O_{22} has a maximum value of σ_{iso} (321.5263); O_{37} has a maximum value of σ_{aniso} (804.3858); O_{37} has a maximum value of Δσ (804.3858), C_{56} has a maximum value of K (0.849443) and C_{46} has a maximum value of η (0.983353) and at HF model with 6-31G(d) basis set O_{22} has a maximum value of σ_{iso} (295.3703); O_{37} has a maximum value of σ_{aniso} (871.3947); O_{37} has a maximum value of Δσ (871.3947), C_{56} has a maximum value of K (0.858789) and O_{22} has a maximum value of η (0.969841). At B3LYP model with 3-21G(d) basis set O_{22} has a maximum value of σ_{iso} (293.5912); O_{37} has a maximum value of σ_{aniso} (697.9934); O_{37} has a maximum value of Δσ (697.9934), C_{56} has a maximum value of K (0.723123), C_{40} has a maximum value of η (0.994685) and at B3LYP model with 6-31G(d) basis set O_{22} has a maximum value of σ_{iso} (269.1406); O_{37} has a maximum value of σ_{aniso} (751.9676); O_{37} has a maximum value of Δσ (751.9676), C_{27} has a maximum value of K (0.725056), C_{43} has a maximum value of η (0.993623). As shown in Figure 2 and 3, at all four used theoretical methods, O_{24}, O_{37}, O_{49} and O_{55} have minimum values of σ_{iso}. Since the σ_{iso} is related to electron density on atoms, therefore these atoms can be considered as active sites of vincristine. The titled molecule can bind to tubulin or microtubule via hydrogen bonding of the mentioned atoms as donors with some hydrogens of target molecular structure. These hydrogen bonds disturb the active structure of tubulin or microtubule leading to decrease or stop in cellular division of cancer cells and finally cell death.

The calculated chemical shifts by HF and B3LYP methods with 3-21G(d) and 6-31G(d) basis sets as compared with experimental data in $CDCl_3$, DMSO and CD_3CN+D_2O (1:1) (Dubrovay *et al.*, 2013) have been compiled in Table 3. The results show that in some cases the data are comparable and in some other ones there is notable difference. These differences may be expectable because the theoretical calculations have been performed in gas phase and the solvent effects have not been considered. Finally, in an overall view, it seems that the NMR data obtained by HF methods are more near to experimental data.

For conformational analysis of the titled compound and finding of probable stable and active conformer, vincristine molecule was rotated around C_{10}-C_{27} bond and then theoretical computations were performed at each status at B3LYP/3-21g level of theory typically. For this mean, we changed the torsion angle around the mentioned bond and then NMR analyses were performed for each torsion angle. Based on these analyses, magnetic shielding tensor (σ, ppm), shielding asymmetry (η), magnetic shielding anisotropy (σ_{aniso}) and skew of a tensor (K) were computed and the

Table 1. Magnetic shielding tensor (σ, ppm), magnetic shielding anisotropy (σ_{aniso}, ppm) calculated by HF and B3LYP model with 3-21G(d) and 6-31G(d) basis set for C, N, O in vincristine.

Atomic label	NMR chemical shielding tensors data							
	HF				B3LYP			
	3-21G(d)		6-31G(d)		3-21G(d)		6-31G(d)	
	σ_{Iso}	σ_{Aniso}	σ_{Iso}	σ_{Aniso}	σ_{Iso}	σ_{Aniso}	σ_{Iso}	σ_{Aniso}
1c	98.0948	161.8528	82.3483	177.837	97.9939	142.5477	81.6205	156.6853
2c	102.0269	157.1853	85.9302	172.4647	98.4149	141.4388	81.4449	154.3576
3c	96.0694	165.8748	79.6685	181.4868	95.8071	144.9129	78.6314	157.7927
4c	108.9115	142.2651	93.5194	156.4156	106.4881	126.916	90.3549	138.827
5c	92.4484	146.9877	74.2558	165.1493	87.9913	132.7228	68.2517	148.8975
6c	84.6551	147.8632	66.1123	164.2468	84.5304	124.994	65.2192	138.9801
7N	159.2039	60.5605	140.9509	66.0882	140.9182	58.2824	120.3577	61.1834
8c	87.0558	108.2597	70.3182	121.3395	84.9748	89.5309	67.0894	100.8703
9c	108.1281	110.4487	91.8312	126.0032	102.1065	97.742	84.6932	110.0943
10c	170.1268	32.6314	160.4131	34.6484	157.5145	31.8566	146.1094	33.1685
11c	169.269	23.882	159.3887	23.8077	151.1823	22.5007	138.3082	22.196
12c	178.9717	29.676	169.3545	31.1189	161.1951	29.18	149.4101	31.0389
13c	184.0953	30.2121	175.2179	31.0146	169.5226	30.7033	158.0084	32.0737

Table 1. Continued

Atomic label	NMR chemical shielding tensors data							
	HF				B3LYP			
	3-21G(d)		6-31G(d)		3-21G(d)		6-31G(d)	
	σ_{Iso}	σ_{Aniso}	σ_{Iso}	σ_{Aniso}	σ_{Iso}	σ_{Aniso}	σ_{Iso}	σ_{Aniso}
14c	152.8674	39.6931	140.8375	47.8963	133.2564	41.7412	119.5313	47.8689
15c	165.6791	28.3975	155.0226	29.7808	150.393	29.6713	137.1109	30.4962
16N	276.7839	70.5591	264.9895	73.1478	246.1696	69.4623	231.312	73.2929
17c	192.6461	21.8915	184.9401	20.7402	180.0918	25.0969	170.6063	24.1922
18c	169.2	44.9863	159.4433	47.9309	154.5289	46.4745	142.428	49.4212
19c	176.3222	33.7229	167.1846	36.3271	161.6308	36.8413	150.1123	39.7194
20c	205.1247	16.3841	199.1436	15.5654	194.6099	17.6737	187.2181	16.223
21c	185.1512	33.362	175.8734	34.598	171.4098	34.4368	159.7531	35.4772
22O	321.5263	55.8681	295.3703	50.1249	293.5912	48.9159	269.1406	42.0477
23c	37.9888	107.2785	13.0062	130.2017	41.3991	75.1399	17.8366	90.9124
24O	-121.0634	701.5065	-166.454	767.0105	-92.9699	613.2515	-130.935	665.9071
25O	211.5951	189.5687	172.4182	208.4978	163.4965	173.8873	125.8576	189.3845
26c	166.6817	59.323	157.7395	63.4683	155.115	62.6906	144.3693	66.4899
27c	90.3559	148.9459	72.087	169.9898	86.3332	132.7497	67.1707	151.2445
28c	64.4195	116.916	45.8541	132.8738	60.023	92.348	40.5371	104.5942
29c	116.6423	126.7701	101.8142	142.3168	114.643	113.631	99.2877	127.5041
30c	90.0485	152.3345	73.5423	168.2952	90.8093	129.93	73.1695	143.4504
31c	91.7148	126.9856	73.4279	145.204	87.5409	109.7434	68.2044	124.9715
32c	74.9429	122.9957	57.5599	136.0929	73.8417	97.8844	55.1121	107.9953
33N	153.2093	89.9138	124.2857	102.1544	118.0281	83.0874	86.5403	95.3261
34c	151.949	23.0924	140.5245	24.148	135.0999	21.7084	120.527	23.4671
35c	165.7432	28.7517	155.1711	28.5767	147.6648	26.2138	134.3469	27.1822
36c	48.0014	112.5763	23.7398	133.91	53.1912	80.8872	30.7528	95.8841
37O	-162.5361	804.3858	-208.706	871.3947	-127.127	697.9934	-165.226	751.9676
38c	39.3436	15.416	127.6873	20.3306	120.9674	19.8958	108.0863	23.0187
39c	147.1483	28.0209	135.7454	31.7208	129.8288	29.4525	115.9112	32.9358
40c	174.7346	13.7432	165.7739	14.9397	156.1838	13.3706	144.8184	14.4124
41c	157.6848	34.6275	146.4887	35.9882	140.8005	37.2364	126.656	39.3115
42c	170.0442	38.2486	160.3444	39.8532	155.0624	40.7634	142.7023	42.5692
43c	87.5433	150.3146	71.7933	166.6598	83.6319	136.7119	66.6303	150.9837
44c	101.3525	129.5564	85.8623	144.1893	95.7113	117.1619	79.285	129.4261
45N	235.6174	37.345	219.5058	37.0874	204.3163	36.8159	184.6121	37.3639
46c	205.8608	12.4891	199.9801	11.4392	195.0253	14.0374	187.6615	12.2918
47c	188.111	27.6709	179.7243	27.754	173.7991	28.2908	162.6295	28.5269
48c	39.9413	103.5205	16.153	123.9514	43.1541	71.843	20.3705	86.0096
49O	-109.9413	678.0923	-155.675	745.3261	-84.2037	590.1872	-122.409	643.1227
50O	204.2318	188.842	164.3097	211.1877	152.3209	166.1997	112.6951	182.4398
51c	167.4309	57.8535	158.2931	62.6972	155.4505	61.4394	144.4035	66.0543
52O	307.5378	60.794	277.6782	64.2559	272.7351	62.3887	244.6268	64.2973
53O	192.7573	173.1545	148.3453	197.2289	145.2709	149.7283	101.9425	169.6354
54c	39.5513	113.2062	14.5616	134.1953	44.1329	79.1269	20.6635	93.7747
55O	-101.9121	658.6248	-140.452	706.829	-84.4772	580.6779	-117.853	620.1751
56c	189.3663	45.0055	180.8292	49.6345	180.9671	44.654	171.3875	47.9222
57c	176.3433	46.01	166.3079	49.5584	63.11	46.1003	151.0356	50.3433
58c	170.6613	53.1666	160.9898	57.0699	155.9579	55.6025	143.9522	60.078
59O	309.8479	81.2607	258.3373	92.8512	267.2494	87.4677	240.8299	98.4738
60c	164.1668	64.2024	154.8109	69.2281	151.7351	69.8599	140.9629	73.7758

Table 2. Skew of a tensor (K) and shielding asymmetry (η) calculated by HF and B3LYP model with 3-21G(d) and 6-31G(d) basis set for C, N, O in vincristine.

Atomic label	NMR chemical shielding tensors data							
	HF				B3LYP			
	3-21G(d)		6-31G(d)		3-21G(d)		6-31G(d)	
	K	η	K	η	K	η	K	η
1c	0.176197	0.778102	0.180191	0.773359	0.215481	0.731943	0.225438	0.720425
2c	0.117181	0.849630	0.121235	0.844631	0.148369	0.811495	0.156328	0.801884
3c	0.161132	0.796108	0.162610	0.794333	0.182964	0.770070	0.187799	0.764352
4c	0.166821	0.789287	0.186285	0.766140	0.218079	0.728931	0.242300	0.701076
5c	0.662957	0.276041	0.648255	0.289242	0.712451	0.232366	0.708994	0.235378
6c	0.389035	0.540831	0.349037	0.583118	0.446755	0.481534	0.407999	0.521126
7N	-0.378257	0.552128	-0.36219	0.569094	-0.37756	0.552856	-0.39742	0.532083
8c	-0.151367	0.807869	-0.15352	0.805263	-0.02612	0.965473	-0.01494	0.980172
9c	0.120739	0.845243	0.143247	0.817705	0.368837	0.562058	0.402378	0.526942
10c	0.302428	0.633693	0.439399	0.488984	0.163878	0.792821	0.299685	0.636713
11c	0.127083	0.837435	0.171557	0.783635	0.123076	0.842358	0.181699	0.771593
12c	0.303868	0.632101	0.217748	0.729320	0.342769	0.589838	0.241245	0.702284
13c	0.338131	0.594829	0.222555	0.723752	0.409495	0.519578	0.326601	0.607281
14c	0.430111	0.498426	0.559023	0.371713	0.377123	0.553319	0.470979	0.457239
15c	0.188891	0.763058	0.129078	0.834994	0.240672	0.702935	0.150124	0.809372
16N	-0.076894	0.900036	-0.04500	0.940878	-0.06827	0.910995	-0.06291	0.917845
17c	-0.636938	0.299492	-0.74235	0.206532	-0.51698	0.412021	-0.60932	0.324715
18c	0.492729	0.435713	0.507948	0.420803	0.426513	0.502104	0.45038	0.477891
19c	0.464759	0.463437	0.451017	0.477238	0.474910	0.453332	0.44671	0.481582
20c	0.477274	0.450978	0.390624	0.539178	0.582289	0.349806	0.41434	0.514571
21c	0.626178	0.309271	0.666219	0.273128	0.584418	0.347823	0.63500	0.301236
22O	0.176200	0.778098	0.022790	0.969841	-0.08901	0.884735	-0.35391	0.577911
23c	-0.669297	0.270380	-0.53529	0.394339	-0.81286	0.147239	-0.67222	0.267773
24O	0.583678	0.348514	0.602627	0.330902	0.536071	0.393596	0.53194	0.397566
25O	-0.631137	0.304749	-0.70363	0.240057	-0.73652	0.211541	-0.76727	0.185326
26c	0.659529	0.279106	0.623975	0.311279	0.587986	0.344494	0.576985	0.354780
27c	0.596664	0.336426	0.624530	0.310772	0.689788	0.252220	0.725056	0.221426
28c	0.032138	0.957604	0.043299	0.943089	0.234241	0.710299	0.216409	0.730871
29c	0.334888	0.598321	0.399492	0.529939	0.395837	0.533739	0.473327	0.454900
30c	0.130059	0.833792	0.159863	0.797631	0.147715	0.812289	0.185417	0.767167
31c	0.278172	0.660575	0.301300	0.634930	0.362606	0.568662	0.397733	0.531765
32c	-0.066650	0.913062	-0.10283	0.867435	-0.03112	0.958923	-0.07398	0.903724
33N	-0.446162	0.482135	-0.53925	0.390541	-0.57736	0.354420	-0.63527	0.300989
34c	-0.622354	0.312762	-0.61536	0.319161	-0.74110	0.207599	-0.69339	0.249041
35c	0.548716	0.381504	0.530802	0.398664	0.59974	0.333573	0.63227	0.303718
36c	-0.608319	0.325648	-0.44979	0.478471	-0.75383	0.196727	-0.59435	0.338568
37O	0.537759	0.391977	0.537344	0.392374	0.457146	0.471070	0.433682	0.494790
38c	0.111472	0.856703	0.379987	0.550314	0.344542	0.587934	0.346033	0.586346
39c	-0.411393	0.517627	-0.35555	0.576157	-0.52516	0.404093	-0.47860	0.449656
40c	0.047311	0.937918	0.060050	0.921504	-0.00398	0.994685	-0.01588	0.978940
41c	0.243626	0.699562	0.304931	0.630941	0.328717	0.604991	0.385724	0.544296
42c	0.374601	0.555972	0.283328	0.654828	0.325391	0.608601	0.284239	0.653813
43c	-0.165025	0.791201	-0.14389	0.816925	-0.03210	0.957646	-0.00479	0.993623
44c	-0.283875	0.654451	-0.25617	0.685309	-0.15675	0.801372	-0.12484	0.840185
45N	-0.696530	0.246283	-0.76187	0.189900	-0.58728	0.345147	-0.65563	0.282605
46c	0.012537	0.983353	-0.06381	0.916660	0.169834	0.785676	0.042888	0.943609

Table 2. Continued

Atomic label	NMR chemical shielding tensors data							
	HF				B3LYP			
	3-21G(d)		6-31G(d)		3-21G(d)		6-31G(d)	
	K	η	K	η	K	η	K	η
47c	0.107969	0.861036	0.057884	0.924275	0.099473	0.871625	0.043984	0.942207
48c	-0.655514	0.282711	-0.52974	0.399676	-0.80625	0.152706	-0.67627	0.264172
49O	0.695812	0.246917	0.708389	0.235905	0.608160	0.325794	0.590840	0.341835
50O	-0.633929	0.302209	-0.70222	0.241293	-0.79971	0.158130	-0.84028	0.124771
51c	0.618094	0.316661	0.592433	0.340354	0.556745	0.373870	0.544488	0.385539
52O	0.075017	0.902414	0.175132	0.779369	0.094764	0.877516	0.041519	0.945393
53O	-0.664394	0.274755	-0.72110	0.224850	-0.82809	0.134719	-0.85634	0.111757
54c	-0.613063	0.321281	-0.48269	0.445612	-0.78825	0.167684	-0.64968	0.287955
55O	0.534679	0.394932	0.530741	0.398720	0.517583	0.411433	0.498833	0.429714
56c	0.849443	0.117332	0.858789	0.109786	0.723123	0.223098	0.712961	0.231919
57c	0.529309	0.400095	0.552830	0.377584	0.572767	0.358745	0.632505	0.313167
58c	0.224240	0.721806	0.265503	0.674780	0.291994	0.645208	0.318639	0.615939
59O	-0.589045	0.343508	-1.07461	0.563103	-0.55680	0.373810	-0.50764	0.421097
60c	0.681146	0.259852	0.649720	0.287924	0.690795	0.251332	0.661713	0.277155

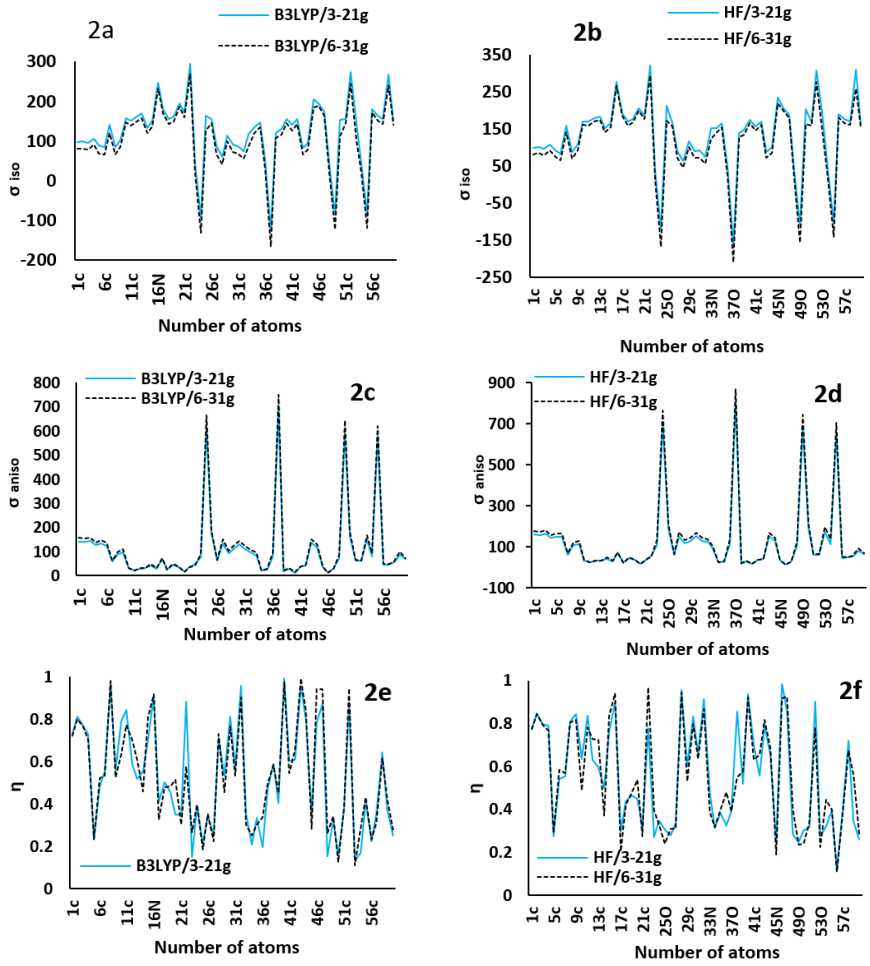

Figure 2. Graphs of a, b) σ_{iso}, c, d) σ_{aniso}, e, f) η versus atoms of vincristine in gas phases at the B3LYP / 3-21G (d), B3LYP / 6-31G (d), HF/ 3-21G (d) and HF/ 6-31G (d) basis set.

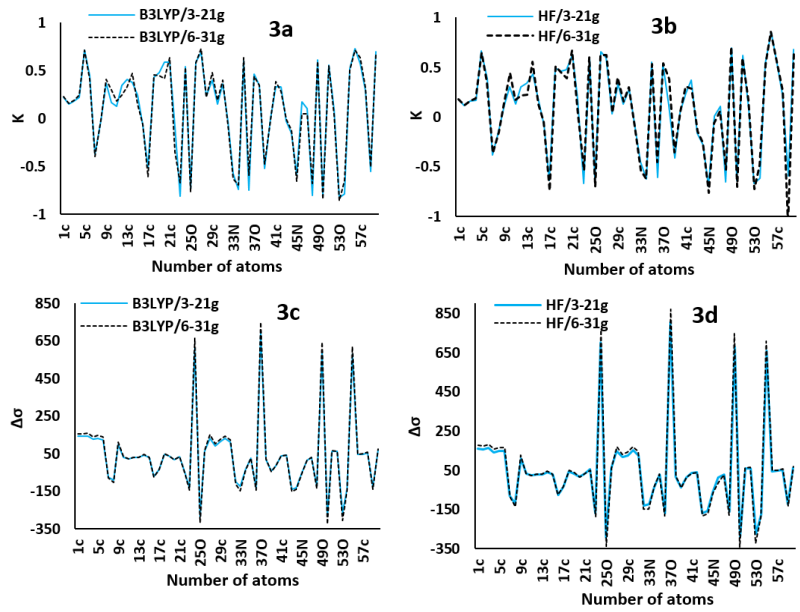

Figure 3. Graphs of a, b) K and c, d) Δσ, versus atoms of vincristine in gas phases at the B3LYP / 3-21G (d), B3LYP / 6-31G (d), HF/ 3-21G (d) and HF/ 6-31G (d) basis set.

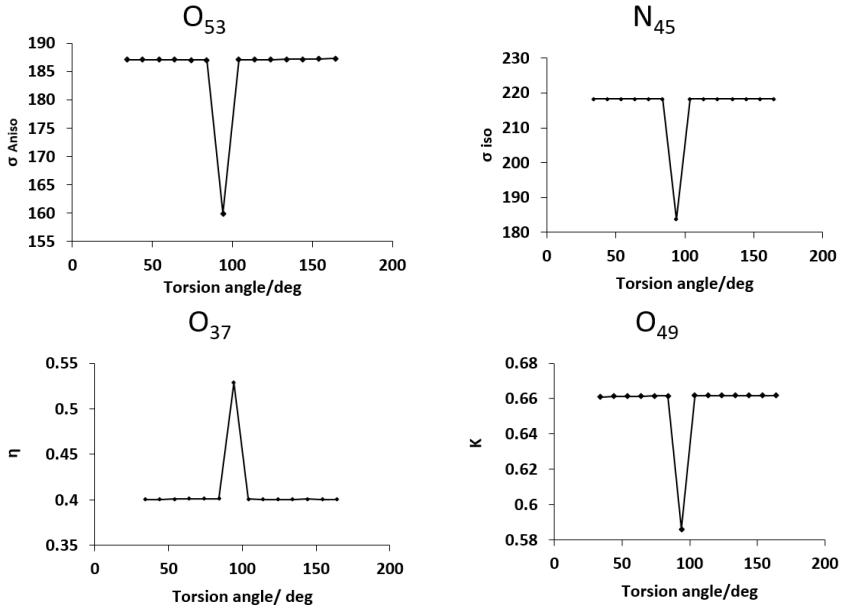

Figure 4. Graphs of σ_{aniso}, σ_{iso}, η and K, versus torsion angles around the C_{10}-C_{27} bond for some atoms of vincristine at B3LYP/3-21g level of theory.

graphs of this calculated parameters versus the torsion angle for some atoms were drawn and some of them as typical have been exhibited in Figure 4. As shown there, skew parameter (k) change versus torsion angles for O_{49} and the plot of shielding asymmetry changes (η) versus torsion angles for O_{37} are found as *Dirac delta* function (positive and negative respectively). The plots of σ_{iso} and σ_{Aniso} versus torsion angles *are also observed as Dirac delta* function with maximum values in torsion angle of 94.3° for N_{45} and O_{53}. It is to be noted that this angle is the one that is found at optimized structure of vincristine. About other atoms, such behaviors are also found. In this way, based on our theoretical results, it is suggested that the conformer with 94.3° around the C_{10}-C_{27} in the structure (Figure 1) is the most stable conformer among many other possible ones.

Moreover, some electronic properties such as energy of the highest occupied molecular orbital (E_{HOMO}), energy of the lowest unoccupied molecular orbital (E_{LUMO}), energy

Table 3. Experimental (in $CDCl_3$, DMSO and $CD_3CN + D_2O$ (1:1)) and calculated chemical shifts by B3LYP and HF model with 3-21G(d) and 6-31G(d) basis set.

^{13}C NMR chemical shift data (δ)							
Atomic label	Calculation				Experimental		
	HF		B3LYP		$CDCL_3$ solvent	DMSO solvent	$CD_3CN + D_2O$ (1:1) solvent
	3-21G(d)	6-31G(d)	3-21G(d)	6-31G(d)			
1c	107.9019	118.5579	95.0319	104.4568	118.7	117.7	118.8
2c	104.7902	114.9764	94.2926	102.9051	119.1	118.0	119.3
3c	110.5832	120.9912	96.6086	105.1951	122.5	121.1	122.7
4c	94.8434	104.2771	84.6107	92.5513	110.8	111.9	111.7
5c	97.9917	110.0995	88.4818	99.265	129.7	128.7	129.8
6c	98.5754	109.4979	83.3294	92.6534	135.3	135.8	136.1
8c	-79.8433	-89.6191	-60.7358	-67.9202	130.2	130.4	130.0
9c	73.6324	84.0022	65.0495	73.3962	118.0	116.0	117.7
10c	21.7542	23.0989	21.2377	22.1123	56.0	55.6	56.2
11c	15.9217	15.8718	15.0005	14.7973	34.0	34.4	35.0
12c	19.784	20.7459	19.4533	20.6926	30.1	29.4	29.3
13c	20.1414	20.6764	20.4689	21.3825	41.3	40.4	39.9
14c	26.4621	31.9308	27.8275	31.9126	69.4	67.2	68.9
15c	18.9317	19.8539	19.7809	20.3308	64.0	63.7	62.5
17c	-22.4613	-22.9199	-23.6983	-24.3496	28.6	27.7	26.9
18c	29.9908	31.9539	30.983	32.9464	55.9	56.2	56.2
19c	22.482	24.2181	24.5608	26.4796	47.6	46.6	46.1
20c	10.9227	10.3769	11.7825	10.8154	6.8	7.0	6.7
21c	22.2413	23.0653	22.9579	23.6515	34.5	34.2	34.7
23c	-112.5946	-124.5049	-87.3282	-95.6138	174.3	174.0	176.2
26c	39.5487	42.3122	41.7937	44.3266	52.6	52.0	52.9
27c	99.2972	113.3266	88.4997	100.8297	128.1	127.6	128.4
28c	77.944	88.5825	61.5653	69.7294	158.0	156.5	158.3
29c	84.5134	94.8779	75.754	85.0027	95.2	95.8	95.5
30c	101.5563	112.1968	86.62	95.6336	124.0	125.0	125.8
31c	84.6571	96.803	73.1622	83.3143	124.0	123.7	124.6
32c	-85.7235	-97.1692	-66.6246	-75.638	141.2	141.0	141.3
34c	-23.4542	-24.4074	-23.9687	-25.0508	72.2	71.3	71.9
35c	19.1678	19.0511	17.4759	18.1214	52.8	52.3	53.2
36c	-113.2289	-120.7644	-90.1204	-95.5091	160.5	161.3	162.6
38c	10.2773	13.5537	13.2639	15.3457	79.7	79.2	79.9
39c	-24.6181	-26.8338	-27.9683	-30.2929	76.8	76.9	77.5
40c	9.1621	9.9598	-8.9375	-9.7105	42.3	41.8	42.6
41c	23.085	23.9921	24.8243	26.2076	64.8	62.7	63.5
42c	25.4991	26.5688	27.1756	28.3795	49.7	49.1	49.9
43c	-111.8746	-122.3017	-93.1131	-100.9777	129.7	130.1	129.7
44c	-104.4283	-114.0755	-86.7205	-93.7776	124.9	124.2	125.9
46c	8.3261	-7.9578	9.3583	8.1946	8.3	7.6	7.9
47c	18.4473	18.5027	18.8605	19.0179	30.8	30.7	31.0
48c	-107.6059	-118.0762	-83.1006	-90.715	170.6	170.1	171.5
51c	38.569	41.7982	40.9596	44.0362	52.9	51.7	53.1
54c	-114.2388	-123.7725	-90.3519	-97.0786	170.4	169.6	171.9
56c	30.0037	33.0896	29.7694	31.9481	21.0	20.7	20.6
57c	30.6734	33.039	30.7335	33.5622	41.5	41.4	41.2
58c	35.4444	38.0466	37.0683	40.052	49.1	48.0	48.6
60c	42.8016	46.152	46.5733	49.1839	56.1	56.5	56.7

Table 4. Some electronic properties of vincristine.

Basis Set	E_{HOMO}(ev)	E_{LUMO}(ev)	Eg; Δ(ev)
HF/3-21g	-0.27896	0.11050	0.38946
HF/6-31g	-0.27907	0.10476	0.38383
B3LYP/3-21g	-0.17836	-0.02112	0.15724
B3LYP/6-31g	-0.18608	-0.02729	0.15879

band gap (E_{bg}) (the gap between LUMO and HOMO energies) and atomic charges, were evaluated and summarized in Table 4. The maximum and minimum values of E_{bg} are found in HF/3-21g and B3LYP/3-21g respectively. Also Mullikan atomic charges were evaluated and were presented in Table 5 and 6. The maximum Mullikan negative charge was evaluated for 7N and the maximum positive charge was found for 48c in HF and B3LYP methods.

Table 5. Calculated Mullikan atomic charges for all atoms in vincristine molecular structure by HF method with 3-21g and 6-31g basis set.

Atomic label	Mullikan Charge HF/3-21g	Mullikan Charge HF/ 6-31g	Atomic label	Mullikan Charge HF/3-21g	Mullikan Charge HF/6-31g	Atomic label	Mullikan Charge HF/3-21g	Mullikan Charge HF/6-31g
1c	-0.2198	-0.13115	40c	-0.29414	-0.14563	79H	0.195917	0.147424
2c	-0.251	-0.22679	41c	0.075334	0.066268	80H	0.225834	0.185375
3c	-0.23301	-0.21655	42c	-0.2023	-0.10567	81H	0.194096	0.145466
4c	-0.23503	-0.12916	43c	-0.067	-0.04698	82H	0.208027	0.156857
5c	-0.14061	-0.22759	44c	-0.25024	-0.19406	83H	0.219019	0.164283
6c	0.408439	0.33612	45N	-0.72193	-0.79656	84H	0.395245	0.428912
7N	-1.03204	-1.06261	46c	-0.62713	-0.48984	85H	0.222536	0.18932
8c	0.413428	0.291821	47c	-0.38505	-0.30717	86H	0.216909	0.182934
9c	-0.01062	0.076926	48c	0.962034	0.845394	87H	0.217332	0.183263
10c	-0.47707	-0.28116	49O	-0.60816	-0.56339	88H	0.271195	0.245576
11c	-0.25112	-0.19273	50O	-0.66617	-0.69842	89H	0.246818	0.22399
12c	-0.27138	-0.1809	51c	-0.28362	-0.14653	90H	0.29591	0.262719
13c	-0.38446	-0.28199	52O	-0.7026	-0.76257	91H	0.209615	0.178685
14c	0.169864	0.221568	53O	-0.67716	-0.71318	92H	0.275828	0.250133
15c	-0.14925	-0.06451	54c	0.857352	0.782404	93H	0.231831	0.178365
16N	-0.72605	-0.7494	55O	-0.61235	-0.57553	94H	0.204184	0.159183
17c	-0.50788	-0.34198	56c	-0.67679	-0.50687	95H	0.235218	0.188624
18c	-0.14271	-0.06492	57c	-0.38708	-0.31737	96H	0.250978	0.209167
19c	-0.15372	-0.07634	58c	-0.18186	-0.06817	97H	0.231071	0.188809
20c	-0.59474	-0.46265	59O	-0.7383	-0.84568	98H	0.173776	0.124013
21c	-0.39066	-0.27747	60c	-0.29842	-0.16258	99H	0.259801	0.231365
22O	-0.68352	-0.77124	61H	0.234901	0.206771	100H	0.206494	0.158514
23c	0.932432	0.799491	62H	0.22989	0.190854	101H	0.235534	0.176874
24O	-0.60153	-0.55929	63H	0.233654	0.193657	102H	0.217693	0.170071
25O	-0.68459	-0.72575	64H	0.231249	0.204424	103H	0.206429	0.172244
26c	-0.28144	-0.14237	65H	0.420611	0.467679	104H	0.216313	0.183826
27c	-0.02874	0.006015	66H	0.325287	0.27754	105H	0.219279	0.186963
28c	0.383411	0.394062	67H	0.284704	0.245075	106H	0.453036	0.51384
29c	-0.27049	-0.18948	68H	0.241178	0.183376	107H	0.244809	0.197039
30c	-0.20757	-0.21748	69H	0.237623	0.190879	108H	0.241083	0.195814
31c	-0.01445	-0.01897	70H	0.228327	0.176213	109H	0.267389	0.222086
32c	0.341708	0.26318	71H	0.237222	0.185035	110H	0.240242	0.196409
33N	-0.8691	-0.81833	72H	0.218883	0.178092	111H	0.228738	0.178858
34c	0.034579	0.029715	73H	0.243846	0.201313	112H	0.205176	0.161098
35c	-0.20469	-0.09654	74H	0.2247	0.173001	113H	0.235567	0.192043
36c	0.613314	0.58378	75H	0.208196	0.161376	114H	0.215423	0.18184
37O	-0.56343	-0.5401	76H	0.205791	0.162693	115H	0.23582	0.198202
38c	0.11346	0.225947	77H	0.199753	0.15812	116H	0.219579	0.180371
39c	0.169842	0.170081	78H	0.210204	0.154184			

4.1 Natural bond orbital analysis

Natural orbitals are applied in computational analyses to compute the distribution of electron density on atoms and in bonds between atoms. The highest possible percentages of the electron density, ideally close to 2.000 are considered in natural bond orbital (NBO) analyses. This is performed by considering all possible interactions between filled donor and empty acceptor NBOs and investigating their energetic importance by second-order perturbation theory. For each donor NBO (i) and acceptor NBO (j), the stabilization energy E (2) associated with electron delocalization between donor and acceptor is calculated by equation of:

$$E^{(2)} = -q_i \frac{(F)^2_{i,j}}{\varepsilon_j - \varepsilon_i}$$

Table 6. Calculated Mullikan atomic charges for all atoms in vincristine molecular structure by B3LYP method with 3-21g and 6-31g basis set.

Atomic label	Mullikan Charge B3LYP/3-21g	Mullikan Charge HF/ B3LYP/6-31g	Atomic label	Mullikan Charge B3LYP/3-21g	Mullikan Charge B3LYP/6-31g	Atomic label	Mullikan Charge B3LYP/3-21g	Mullikan Charge B3LYP/6-31g
1c	-0.22699	-0.14084	40c	-0.21828	-0.02666	79H	0.183565	0.125229
2c	-0.18863	-0.13675	41c	0.024789	0.016883	80H	0.205903	0.158684
3c	-0.1919	-0.15532	42c	-0.24589	-0.13957	81H	0.18595	0.130765
4c	-0.19551	-0.07784	43c	-0.04426	-0.01664	82H	0.191802	0.129171
5c	-0.03538	-0.07568	44c	-0.19003	-0.11962	83H	0.198306	0.131711
6c	0.364839	0.275498	45N	-0.54435	-0.55869	84H	0.357796	0.376092
7N	-0.86234	-0.81748	46c	-0.59776	-0.44382	85H	0.214136	0.170817
8c	0.366228	0.234093	47c	-0.36358	-0.272	86H	0.210521	0.166983
9c	0.042527	0.138958	48c	0.744964	0.556444	87H	0.206524	0.159908
10c	-0.44401	-0.23233	49O	-0.48326	-0.409	88H	0.208531	0.154199
11c	-0.25973	-0.19132	50O	-0.49691	-0.48578	89H	0.18696	0.138196
12c	-0.21722	-0.1001	51c	-0.33111	-0.17821	90H	0.249037	0.195402
13c	-0.35788	-0.24213	52O	-0.58391	-0.61422	91H	0.174769	0.124523
14c	0.133605	0.194453	53O	-0.50747	-0.49314	92H	0.234156	0.187866
15c	-0.18946	-0.10646	54c	0.658146	0.537062	93H	0.207068	0.130514
16N	-0.54597	-0.50487	55O	-0.48163	-0.41672	94H	0.193935	0.135798
17c	-0.51065	-0.33613	56c	-0.63965	-0.45686	95H	0.218535	0.15818
18c	-0.18359	-0.09909	57c	-0.3618	-0.28004	96H	0.200743	0.138799
19c	-0.20448	-0.12514	58c	-0.20617	-0.08392	97H	0.189673	0.128891
20c	-0.5682	-0.41646	59O	-0.57112	-0.61899	98H	0.169129	0.114248
21c	-0.35616	-0.22542	60c	-0.34235	-0.18707	99H	0.225991	0.190126
22O	-0.56067	-0.61834	61H	0.174408	0.119899	100H	0.192604	0.136146
23c	0.719897	0.51481	62H	0.174855	0.111796	101H	0.218703	0.148877
24O	-0.47797	-0.40599	63H	0.177488	0.113981	102H	0.198856	0.139624
25O	-0.51068	-0.50647	64H	0.17003	0.116384	103H	0.197494	0.151269
26c	-0.32994	-0.17489	65H	0.346646	0.363749	104H	0.209172	0.167195
27c	0.062476	0.138973	66H	0.272707	0.2085	105H	0.211042	0.169282
28c	0.272646	0.229706	67H	0.240688	0.182818	106H	0.378287	0.414686
29c	-0.20954	-0.10843	68H	0.213835	0.137837	107H	0.226849	0.172389
30c	-0.227	-0.25267	69H	0.209987	0.149984	108H	0.221164	0.167707
31c	0.087293	0.121669	70H	0.205206	0.138494	109H	0.243031	0.191825
32c	0.288407	0.186872	71H	0.218472	0.152011	110H	0.218155	0.162254
33N	-0.67405	-0.55089	72H	0.199917	0.142655	111H	0.209668	0.146021
34c	-0.02051	-0.04336	73H	0.212561	0.15793	112H	0.190464	0.131951
35c	-0.17578	-0.04648	74H	0.202462	0.136435	113H	0.217168	0.160262
36c	0.428376	0.367058	75H	0.195914	0.135949	114H	0.211398	0.168014
37O	-0.43844	-0.39049	76H	0.190383	0.132311	115H	0.223382	0.172899
38c	0.088955	0.213556	77H	0.18418	0.127767	116H	0.215972	0.166412
39c	0.101149	0.083068	78H	0.201711	0.131773			

where q_i is the orbital occupancy, ε_i, ε_j are diagonal elements, and $F_{i,j}$ is the off-diagonal NBO Fock matrix element (Ghiasi *et al.*, 2012).

The aim of the present work is the investigation of the bonding nature in vincristine (Scheme 1), by using natural bond orbital analyses. We expect that the results obtained via NBO calculations can lead to useful insight into the electronic structure of this molecule. The results of NBOs analysis at the HF level of theory with 6-31G(d) basis set have been listed in Table 7.

Table 4 collects the second-order perturbation estimates of 'donor- acceptor' interactions. The results have been obtained by considering all possible interactions between 'filled' (donor) Lewis-type NBOs and 'empty' (acceptor) non-Lewis NBOs, and evaluating their energetic importance by 2nd-order perturbation theory. Since these interactions lead to loss of occupancy from the localized NBOs of the idealized Lewis structure into the empty non-Lewis orbitals (and thus, to departures from the idealized Lewis structure description), they are referred to as 'delo-

Table 7. Results of NBOs analysis at the HF level of theory with 6-31 G(d) basis set.

$Bond^{BD}_{No.\ ele}$	Coefficients hybrids	$E_{acceptor(j)}$-$E_{Doner(i)*}$ Fack Matrix ($F_{i,j}$, a.u.)	E^2 (Kcal/mol)
$C1-C2^{\sigma}_{1.97859}$	$0.7101\ SP^{1.76}+0.7041\ SP^{1.78}$	$\|\Psi\rangle = BD(1)\text{-}BD^{*}(1) = 1.71*0.086$	5.44
$C1-C2^{\pi}_{1.75084}$	$0.6930\ SP+0.7210\ SP$	$\|\Psi\rangle = BD(2)\text{-}BD^{*}(2) = 0.51*0.126$	38.18
$C1-C5^{\sigma}_{1.97319}$	$0.6973\ SP^{1.93}+0.7168\ SP^{1.77}$	$\|\Psi\rangle = BD(1)\text{-}BD^{*}(1) = 1.68*0.095$	6.73
$C1-H61^{\sigma}_{1.98216}$	$0.7875\ SP^{2.38}+0.6163\ S$	$\|\Psi\rangle = BD(1)\text{-}BD^{*}(1) = 1.53*0.078$	5.02
$C2-C3^{\sigma}_{1.97886}$	$0.7059\ SP^{1.91}+0.7083\ SP^{1.88}$	$\|\Psi\rangle = BD(1)\text{-}BD^{*}(1) = 1.79*0.078$	4.20
$C2-H62^{\sigma}_{1.98290}$	$0.7876\ SP^{2.37}+0.6161\ S$	$\|\Psi\rangle = BD(1)\text{-}BD^{*}(1) = 1.58*0.074$	4.38
$C3-C4^{\sigma}_{1.97716}$	$0.7031\ SP^{1.79}+0.7111\ SP^{1.75}$	$\|\Psi\rangle = BD(1)\text{-}BD^{*}(1) = 1.65*0.098$	7.27
$C3-C4^{\pi}_{1.75623}$	$0.6956\ SP+0.7184\ SP$	$\|\Psi\rangle = BD(2)\text{-}BD^{*}(2) = 0.50*0.124$	35.09
$C3-H63^{\sigma}_{1.98273}$	$0.7878\ SP^{2.39}+0.6159\ S$	$\|\Psi\rangle = BD(1)\text{-}BD^{*}(1) = 1.54*0.080$	5.20
$C4-C6^{\sigma}_{1.97533}$	$0.6974\ SP^{1.99}+0.7167\ SP^{1.60}$	$\|\Psi\rangle = BD(1)\text{-}BD^{*}(1) = 1.77*0.98$	6.75
$C4-H64^{\sigma}_{1.98243}$	$0.7878\ SP^{2.32}+0.6159\ S$	$\|\Psi\rangle = BD(1)\text{-}BD^{*}(1) = 1.55*0.078$	4.95
$C5-C6^{\sigma}_{1.96449}$	$0.7073\ SP^{2.25}+0.7269\ SP^{1.94}$	$\|\Psi\rangle = BD(1)\text{-}BD^{*}(1) = 1.74*0.087$	6.18
$C5-C6^{\pi}_{1.62766}$	$0.7279\ SP+0.6857\ SP$	$\|\Psi\rangle = BD(2)\text{-}BD^{*}(2) = 0.49*0.128$	40.31
$C5-C9^{\sigma}_{1.96386}$	$0.7123\ SP^{2.02}+0.7019\ SP^{2.28}$	$\|\Psi\rangle = BD(1)\text{-}BD^{*}(1) = 1.46*0.105$	9.39
$C6-N7^{\sigma}_{1.98396}$	$0.6226\ SP^{2.64}+0.7826\ SP^{1.90}$	$\|\Psi\rangle = BD(1)\text{-}BD^{*}(1) = 1.86*0.071$	3.34
$N7-C8^{\sigma}_{1.98086}$	$0.7864\ SP^{2.04}+0.6177\ SP^{2.89}$	$\|\Psi\rangle = BD(1)\text{-}BD^{*}(1) = 1.83*0.090$	5.59
$N7-H65^{\sigma}_{1.98459}$	$0.8657\ SP^{2.26}+0.5006\ S$	$\|\Psi\rangle = BD(1)\text{-}BD^{*}(1) = 1.71*0.053$	2.06
$C8-C9^{\sigma}_{1.97191}$	$0.7089\ SP^{1.48}+0.7053\ SP^{1.81}$	$\|\Psi\rangle = BD(1)\text{-}BD^{*}(1) = 1.58*0.085$	5.78
$C8-C9^{\pi}_{1.87696}$	$0.6961\ SP^{99.99}+0.7179\ SP^{99.99}$	$\|\Psi\rangle = BD(2)\text{-}BD^{*}(2) = 0.52*0.109$	24.13
		$\|\Psi\rangle = BD(2)\text{-}BD^{*}(1) = 0.90*0.036$	4.67
$C8-C10^{\sigma}_{1.97372}$	$0.7008\ SP^{1.94}+0.7133\ SP^{2.68}$	$\|\Psi\rangle = BD(1)\text{-}BD^{*}(1) = 1.33*0.058$	3.04
$C9-C17^{\sigma}_{1.97751}$	$0.7168\ SP^{1.95}+6973\ SP^{2.76}$	$\|\Psi\rangle = BD(1)\text{-}BD^{*}(1) = 1.73*0.095$	6.48
$C10-C11^{\sigma}_{1.97077}$	$0.7176\ SP^{2.70}+0.6965\ SP^{2.93}$	$\|\|\Psi\rangle = BD(1)\text{-}BD^{*}(1) = 1.59*0.054$	2.26
		$\|\Psi\rangle = BD(1)\text{-}BD^{*}(2) = 1.00*0.048$	2.61
$C10-C23^{\sigma}_{1.97514}$	$0.7119\ SP^{3.32}+0.7023\ SP^{1.53}$	$\|\Psi\rangle = BD(1)\text{-}BD^{*}(1) = 1.32*0.064$	3.88
		$\|\Psi\rangle = BD(1)\text{-}BD^{*}(2) = 1.07*0.030$	0.94
$C10-H66^{\sigma}_{1.95700}$	$0.8086\ SP^{3.41}+0.5884\ S$	$\|\Psi\rangle = BD(1)\text{-}BD^{*}(1) = 1.27*0.055$	2.96
		$\|\Psi\rangle = BD(1)\text{-}BD^{*}(2) = 0.85*0.078$	8.56

Table 7. Continued

$Bond^{BD}_{No.\ ele}$	Coefficients hybrids	$E_{acceptor(j)}$-$E_{Doner(i)*}$ Fack Matrix ($F_{i,j}$, a.u.)	E^2 (Kcal/mol)
$C11-C12^{\sigma}_{1.97173}$	$0.7148\ SP^{2.77}+0.6993\ SP^{2.87}$	$\|\Psi>= BD(1)-BD^{*}(1)=1.36*0.046$	1.96
		$\|\Psi>= BD(1)-BD^{*}(2)=0.91*0.051$	3.01
$C11-C27^{\sigma}_{1.97189}$	$0.6970\ SP^{2.88}+0.7170\ SP^{2.12}$	$\|\Psi>= BD(1)-BD^{*}(1)=1.67*0.069$	3.56
$C11-H67^{\sigma}_{1.97140}$	$0.7999\ SP^{3.48}+0.6001\ S$	$\|\Psi>= BD(1)-BD^{*}(1)=1.29*0.072$	4.98
		$\|\Psi>= BD(1)-BD^{*}(2)=0.82*0.041$	2.15
$C12-C13^{\sigma}_{1.98105}$	$0.7147\ SP^{2.75}+0.6994\ SP^{2.87}$	$\|\Psi>= BD(1)-BD^{*}(1)=1.48*0.037$	1.17
$C12-C19^{\sigma}_{1.98228}$	$0.7101\ SP^{2.93}+0.7041\ SP^{2.58}$	$\|\Psi>= BD(1)-BD^{*}(1)=1.38*0.053$	2.51
$C12-H68^{\sigma}_{1.97476}$	$0.7895\ SP^{3.53}+0.6138\ S$	$\|\Psi>= BD(1)-BD^{*}(1)=1.22*0.076$	5.94
$C13-C14^{\sigma}_{1.97677}$	$0.7092\ SP^{2.81}+0.7051\ SP^{2.76}\|$	$\Psi>= BD(1)-BD^{*}(1)=1.34*0.056$	2.97
$C13-H69^{\sigma}_{1.97964}$	$0.7897\ SP^{3.15}+0.6135\ S$	$\|\Psi>= BD(1)-BD^{*}(1)=1.39*0.052$	2.40
$C13-H70^{\sigma}_{1.98267}$	$0.7889\ SP^{3.21}+0.6145\ S$	$\|\Psi>= BD(1)-BD^{*}(1)=1.25*0.058$	3.32
$C14-C15^{\sigma}_{1.97858}$	$0.7071\ SP^{2.76}+0.7071\ SP^{2.69}$	$\|\Psi>= BD(1)-BD^{*}(1)=1.38*0.056$	2.83
$C14-C21^{\sigma}_{1.97500}$	$0.7156\ SP^{2.64}+0.6985\ SP^{2.78}$	$\|\Psi>= BD(1)-BD^{*}(1)=1.36*0.059$	3.15
$C14-O22^{\sigma}_{1.99254}$	$0.5629\ SP^{4.20}+0.8265\ SP^{2.10}$	$\|\Psi>= BD(1)-BD^{*}(1)=1.79*0.044$	1.36
$C15-N16^{\sigma}_{1.98674}$	$0.6225\ SP^{3.40}+0.7826\ SP^{2.26}$	$\|\Psi>= BD(1)-BD^{*}(1)=1.49*0.047$	1.85
$C15-H71^{\sigma}_{1.98279}$	$0.7881\ SP^{2.88}+0.6155\ S$	$\|\Psi>= BD(1)-BD^{*}(1)=1.18*0.079$	6.66
$C15-H72^{\sigma}_{1.98353}$	$0.7870\ SP^{3.10}+0.6169\ S$	$\|\Psi>= BD(1)-BD^{*}(1)=1.25*0.065$	4.23
$N16-C18^{\sigma}_{1.98702}$	$0.7850\ SP^{2.26}+0.6195\ SP^{3.28}$	$\|\Psi>= BD(1)-BD^{*}(1)=1.48*0.052$	2.26
$N16-C19^{\sigma}_{1.98792}$	$0.7771\ SP^{2.33}+0.6294\ SP^{3.25}$	$\|\Psi>= BD(1)-BD^{*}(1)=1.61*0.041$	1.30
$C17-C18^{\sigma}_{1.98348}$	$0.7113\ SP^{2.92}+0.7029\ SP^{2.58}$	$\|\Psi>= BD(1)-BD^{*}(1)=1.43*0.038$	1.27
		$\|\Psi>= BD(1)-BD^{*}(2)=0.97*0.056$	3.60
$C17-H73^{\sigma}_{1.98294}$	$0.7925\ SP^{3.10}+0.6099\ S$	$\|\Psi>= BD(1)-BD^{*}(1)=1.45*0.076$	4.99
		$\|\Psi>= BD(1)-BD^{*}(2)=0.88*0.023$	0.66
$C17-H74^{\sigma}_{1.97866}$	$0.7897\ SP^{3.26}+0.6136\ S$	$\|\Psi>= BD(1)-BD^{*}(1)=1.60*0.076$	4.54
		$\|\Psi>= BD(1)-BD^{*}(2)=0.87*0.039$	1.95
$C18-H75^{\sigma}_{1.98513}$	$0.7839\ SP^{3.09}+0.6209\ S$	$\|\Psi>= BD(1)-BD^{*}(1)=1.26*0.069$	4.77
$C18-H76^{\sigma}_{1.98506}$	$0.7846\ SP^{3.12}+0.6200\ S$	$\|\Psi>= BD(1)-BD^{*}(1)=1.340.067$	4.23
$C19-H77^{\sigma}_{1.98626}$	$0.7836\ SP^{3.22}+0.6213\ S$	$\|\Psi>= BD(1)-BD^{*}(1)=1.27*0.043$	1.80
$C19-H78^{\sigma}_{1.98649}$	$0.7803\ SP^{3.02}+0.6254\ S$	$\|\Psi>= BD(1)-BD^{*}(1)=1.29*0.056$	3.09
$C20-C21^{\sigma}_{1.99079}$	$0.7020\ SP^{2.71}+0.7122\ SP^{2.75}$	$\|\Psi>= BD(1)-BD^{*}(1)=1.35*0.050$	2.26
$C20-H79^{\sigma}_{1.99036}$	$0.7840\ SP^{3.13}+0.6208\ S$	$\|\Psi>= BD(1)-BD^{*}(1)=1.260.067$	4.48
$C20-H80^{\sigma}_{1.99145}$	$0.7902\ SP^{3.06}+0.6128\ S$	$\|\Psi>= BD(1)-BD^{*}(1)=1.38*0.061$	3.34
$C20-H81^{\sigma}_{1.99199}$	$0.7817\ SP^{3.14}+0.6237\ S$	$\|\Psi>= BD(1)-BD^{*}(1)=1.39*.059$	3.11
$C21-H82^{\sigma}_{1.98262}$	$0.7858\ SP^{3.27}+0.6185\ S$	$\|\Psi>= BD(1)-BD^{*}(1)=1.17*0.071$	5.32
$C21-H83^{\sigma}_{1.98349}$	$0.7877\ SP^{3.27}+0.6161\ S$	$\|\Psi>= BD(1)-BD^{*}(1)=1.25*0.066$	4.37
$O22-H84^{\sigma}_{1.99015}$	$0.8667\ SP^{3.96}+0.4988\ S$	$\|\Psi>= BD(1)-BD^{*}(1)=1.51*0.064$	3.42
$C23-O24^{\sigma}_{1.99664}$	$0.5805\ SP^{2.02}+0.8143\ SP^{1.46}$	$\|\Psi>= BD(1)-BD^{*}(1)=1.98*0.044$	1.20

Table 7. Continued

$Bond^{BD}_{No.\ ele}$	Coefficients hybrids	$E_{acceptor(j)}$-$E_{Doner(i)*}$ Fack Matrix ($F_{i,j}$, a.u.)	E^2 (Kcal/mol)
$C23-O24^{\pi}_{1.99186}$	$0.5345\ SP^{99.99}+0.8451\ SP^{99.99}$	$\|\Psi>=BD(1)-BD^{*}(1)=1.31*0.040$	1.54
$C23-O25^{\sigma}_{1.99232}$	$0.5536\ SP^{2.72}+0.8328\ SP^{2.38}$	$\|\Psi>=BD(1)-BD^{*}(1)=1.78*0.044$	1.38
$O25-C26^{\sigma}_{1.99300}$	$0.8361\ SP^{2.41}+0.5486\ SP^{3.93}$	$\|\Psi>=BD(1)-BD^{*}(1)=1.63*0.065$	3.20
$C26-H85^{\sigma}_{1.99627}$	$0.7854\ SP^{2.71}+0.6190\ S$	$\|\Psi>=BD(1)-RY^{*}(1)=2.21*0.030$	0.51
$C26-H86^{\sigma}_{1.99618}$	$0.7841\ SP^{2.72}+0.6206\ S$	$\|\Psi>=BD(1)-RY^{*}(1)=2.21*0.031$	0.53
$C26-H87^{\sigma}_{1.99214}$	$0.7842\ SP^{2.85}+0.6205\ S$	$\|\Psi>=BD(1)-BD^{*}(1)=1.22*0.063$	3.85
$C27-C28^{\sigma}_{1.97253}$	$0.7089\ SP^{1.91}+0.7053\ SP^{1.61}$	$\|\Psi>=BD(1)-BD^{*}(1)=1.76*.090$	5.73
$C27-C28^{\pi}_{1.65774}$	$0.7197\ SP+0.6942\ SP$	$\|\Psi>=BD(2)-BD^{*}(2)=0.50*0.134$	45.19
		$\|\Psi>=BD(2)-BD^{*}(1)=0.91*0.055$	3.44
$C27-C30^{\sigma}_{1.96759}$	$0.7092\ SP^{1.97}+0.7050\ SP^{1.83}$	$\|\Psi>=BD(1)-BD^{*}(1)=1.81*0.094$	6.09
$C28-C29^{\sigma}_{1.97429}$	$0.7055\ SP^{1.63}+0.7087\ SP^{1.92}$	$\|\Psi>=BD(1)-BD^{*}(1)=1.78*0.096$	6.55
$C28-O59^{\sigma}_{1.99193}$	$0.5627\ SP^{3.24}+0.8267\ SP^{2.14}\|$	$\Psi>=BD(1)-BD^{*}(1)=1.96*0.053$	1.81
$C29-C32^{\sigma}_{1.97047}$	$0.7019\ SP^{1.81}+0.7123\ SP^{1.64}$	$\|\Psi>=BD(1)-BD^{*}(1)=1.82*0.106$	7.78
$C29-C32^{\pi}_{1.68658}$	$0.7396\ SP^{99.99}+0.6731\ SP^{99.99}$	$\|\Psi>=BD(2)-BD^{*}(2)=0.50*0.136$	45.26
		$\|\Psi>=BD(2)-BD^{*}(1)=0.94*0.035$	1.44
$C29-H88^{\sigma}_{1.97708}$	$0.7926\ SP^{2.32}+0.6097\ S$	$\|\Psi>=BD(1)-BD^{*}(1)=1.55*0.079$	5.01
$C30-C31^{\sigma}_{1.96987}$	$0.6993\ SP^{1.80}+0.7148\ SP^{1.71}$	$\|\Psi>=BD(1)-BD^{*}(1)=1.80*0.103$	7.35
$C30-C31^{\pi}_{1.68552}$	$0.6886\ SP+0.7252\ SP$	$\|\Psi>=BD(2)-BD^{*}(2)=0.48*0.138$	47.70
		$\|\Psi>=BD(2)-BD^{*}(1)=0.90*0.053$	3.42
$C30-H89^{\sigma}_{1.97920}$	$0.7892\ SP^{2.44}+0.6141\ S$	$\|\Psi>=BD(1)-BD^{*}(1)=1.57*0.085$	5.78
$C31-C32^{\sigma}_{1.96645}$	$0.7068\ SP^{2.13}+0.7074\ SP^{1.85}$	$\|\Psi>=BD(1)-BD^{*}(1)=1.80*0.102$	7.21
$C31-C35^{\sigma}_{1.96520}$	$0.7074\ SP^{2.21}+0.7068\ SP^{2.86}$	$\|\Psi>=BD(1)-BD^{*}(1)=1.70*0.089$	5.78
$C32-N33^{\sigma}_{1.98041}$	$0.6267\ SP^{2.72}+0.7793\ SP^{2.19}$	$\|\Psi>=BD(1)-BD^{*}(1)=1.85*0.067$	3.03
$N33-C34^{\sigma}_{1.98083}$	$0.7913\ SP^{2.27}+0.6114\ SP^{3.77}$	$\|\Psi>=BD(1)-BD^{*}(1)=1.79*0.084$	5.00
$N33-C36^{\sigma}_{1.98426}$	$0.8018\ SP^{2.43}+0.5976\ SP^{2.20}$	$\|\Psi>=BD(1)-BD^{*}(2)=1.13*0.045$	1.86
		$\|\Psi>=BD(1)-BD^{*}(1)=1.83*0.042$	1.22
$C34-C35^{\sigma}_{1.97232}$	$0.7017\ SP^{2.75}+0.7125\ SP^{3.13}$	$\|\Psi>=BD(1)-BD^{*}(1)=1.66*0.082$	5.03
$C34-C38^{\sigma}_{1.97238}$	$0.7078\ SP^{2.75}+0.7064\ SP^{2.65}$	$\|\Psi>=BD(1)-BD^{*}(1)=1.29*0.066$	4.22
$C34-H90^{\sigma}_{1.97919}$	$0.8053\ SP^{2.90}+0.5929\ S$	$\|\Psi>=BD(1)-BD^{*}(1)=1.24*0.058$	3.36
$C35-C41^{\sigma}_{1.96780}$	$0.7131\ SP^{2.98}+0.7011\ SP^{2.85}$	$\|\Psi>=BD(1)-BD^{*}(2)=0.96*0.041$	1.86
		$\|\Psi>=BD(1)-BD^{*}(1)=1.36*0.063$	3.65
$C35-C57^{\sigma}_{1.96847}$	$0.7215\ SP^{3.04}+0.6924\ SP^{2.90}$	$\|\Psi>=BD(1)-BD^{*}(2)=0.96*0.049$	2.75
		$\|\Psi>=BD(1)-BD^{*}(1)=1.36*0.065$	3.86
$C36-O37^{\sigma}_{1.99662}$	$0.5607\ SP^{7.29}+0.8280\ SP^{5.95}$	$\|\Psi>=BD(1)-BD^{*}(1)=1.25*0.028$	0.73
$C36-O37^{\pi}_{1.99474}$	$0.5730\ SP^{3.57}+0.8196\ SP^{2.84}$	$\|\Psi>=BD(2)-BD^{*}(1)=1.70*0.050$	1.85
$C36-H91^{\sigma}_{1.98601}$	$0.7744\ SP^{1.85}+0.6327\ S$	$\|\Psi>=BD(1)-BD^{*}(1)=1.30*0.072$	4.99
$C38-C39^{\sigma}_{1.97396}$	$0.7101\ SP^{2.71}+0.7041\ SP^{2.68}$	$\|\Psi>=BD(1)-BD^{*}(1)=1.65*0.049$	1.80
		$\|\Psi>=BD(1)-BD^{*}(2)=0.98*0.046$	2.55

Table 7. Continued

$Bond^{BD}_{No.\ ele}$	Coefficients hybrids	$E_{acceptor(j)}$-$E_{Doner(i)*}$ Fack Matrix ($F_{i,j}$, a.u.)	E^2 (Kcal/mol)
$C38-C48^{\sigma}_{1.97218}$	$0.7152\,SP^{3.18}+0.6989\,SP^{1.60}$	$\|\Psi>=BD(1)-BD^{*}(1)=1.34*0.064$	3.77
$C38-O52^{\sigma}_{1.98888}$	$0.5952\,SP^{3.65}+0.8036\,SP^{2.59}$	$\|\Psi>=BD(1)-BD^{*}(1)=1.57*0.049$	1.94
		$\|\Psi>=BD(1)-BD^{*}(2)=1.22*0.045$	1.94
$C39-C40^{\sigma}_{1.96782}$	$0.7047\,SP^{2.60}+0.7095\,SP^{3.13}$	$\|\Psi>=BD(1)-BD^{*}(1)=1.40*0.055$	2.67
		$\|\Psi>=BD(1)-BD^{*}(2)=1.03*0.041$	2.06
$C39-O53^{\sigma}_{1.98901}$	$0.5536\,SP^{4.25}+0.8328\,SP^{2.19}$	$\|\Psi>=BD(1)-BD^{*}(1)=1.67*0.058$	2.52
$C39-H92^{\sigma}_{1.97853}$	$0.7983\,SP^{2.84}+0.6023\,S$	$\|\Psi>=BD(1)-BD^{*}(1)=1.23*0.073$	5.49
$C40-C41^{\sigma}_{1.97147}$	$0.7028\,SP^{3.00}+0.7114\,SP^{2.54}$	$\|\Psi>=BD(1)-BD^{*}(1)=1.29*0.047$	2.16
$C40-C43^{\sigma}_{1.96941}$	$0.7213\,SP^{2.96}+0.6926\,SP^{2.23}$	$\|\Psi>=BD(1)-BD^{*}(1)=1.80*0.078$	4.26
$C40-C47^{\sigma}_{1.96949}$	$0.7251\,SP^{2.92}+0.6887\,SP^{2.84}$	$\|\Psi>=BD(1)-BD^{*}(1)=1.31*0.052$	2.53
		$\|\Psi>=BD(1)-BD^{*}(2)=1.01*0.049$	3.00
$C41-N45^{\sigma}_{1.98036}$	$0.6234\,SP^{3.76}+0.7819\,SP^{2.61}$	$\|\Psi>=BD(1)-BD^{*}(1)=1.55*0.061$	2.99
$C41-H93^{\sigma}_{1.98131}$	$0.7886\,SP^{3.03}+0.6149\,S$	$\|\Psi>=BD(1)-BD^{*}(1)=1.24*0.068$	4.61
$C42-C44^{\sigma}_{1.98059}$	$0.7153\,SP^{2.61}+0.6988\,SP^{2.29}$	$\|\Psi>=BD(1)-BD^{*}(1)=1.57*0.073$	4.30
$C42-N45^{\sigma}_{1.98533}$	$0.6143\,SP^{3.47}+0.7890\,SP^{2.47}$	$\|\Psi>=BD(1)-BD^{*}(1)=1.67*0.050$	1.89
$C42-H94^{\sigma}_{1.98387}$	$0.7833\,SP^{2.99}+0.6216\,S$	$\|\Psi>=BD(1)-BD^{*}(1)=1.34*0.026$	0.62
		$\|\Psi>=BD(1)-BD^{*}(2)=0.95*0.058$	4.50
$C42-H95^{\sigma}_{1.98204}$	$0.7902\,SP^{3.01}+0.6128\,S\|$	$\Psi>=BD(1)-BD^{*}(1)=1.23*0.066$	4.42
		$\|\Psi>=BD(1)-BD^{*}(2)=0.94*0.044$	2.53
$C43-C44^{\sigma}_{1.98225}$	$0.7082\,SP^{1.53}+0.7060\,SP^{1.52}$	$\|\Psi>=BD(1)-BD^{*}(1)=1.05*0.061$	4.37
$C43-C44^{\pi}_{1.96962}$	$0.6968\,SP+0.7172\,SP$	$\|\Psi>=BD(1)-BD^{*}(1)=1.33*0.093$	8.23
$C43-H96^{\sigma}_{1.97715}$	$0.7938\,SP^{2.40}+0.6081\,S$	$\|\Psi>=BD(1)-BD^{*}(1)=1.32*0.095$	8.50
$C44-H97^{\sigma}_{1.97896}$	$0.7881\,SP^{2.33}+0.6155\,S$	$\|\Psi>=BD(1)-BD^{*}(1)=1.48*0.057$	2.74
$N45-C58^{\sigma}_{1.98582}$	$0.7875\,SP^{2.60}+0.6163\,SP^{3.53}$	$\|\Psi>=BD(1)-BD^{*}(1)=1.48*0.057$	2.74
$C46-C47^{\sigma}_{1.99044}$	$0.6990\,SP^{2.75}+0.7151\,SP^{2.71}$	$\|\Psi>=BD(1)-BD^{*}(1)=1.32*0.048$	2.18
$C46-H98^{\sigma}_{1.99125}$	$0.7773\,SP^{3.20}+0.6292\,S$	$\|\Psi>=BD(1)-BD^{*}(1)=1.39*0.058$	3.09
$C46-H99^{\sigma}_{1.98805}$	$0.7992\,SP^{2.96}+0.6011\,S$	$\|\Psi>=BD(1)-BD^{*}(1)=1.23*0.072$	5.31
$C46-H100^{\sigma}_{1.99119}$	$0.7853\,SP^{3.12}+0.6191\,S$	$\|\Psi>=BD(1)-BD^{*}(1)=1.39*0.060$	3.24
$C47-H101^{\sigma}_{1.98345}$	$0.7871\,SP^{3.23}+0.6168\,S$	$\|\Psi>=BD(1)-BD^{*}(1)=1.30*0.062$	3.70
$C47-H102^{\sigma}_{1.98234}$	$0.7882\,SP^{3.29}+0.6154\,S$	$\|\Psi>=BD(1)-BD^{*}(1)=1.38*0.064$	3.67
$C48-O49^{\sigma}_{1.99725}$	$0.5798\,SP^{1.91}+0.8148\,SP^{1.39}$	$\|\Psi>=BD(1)-BD^{*}(1)=1.97*0.046$	1.31
$C48-O49^{\pi}_{1.99323}$	$0.5360\,SP^{99.99}+0.8442\,SP^{99.99}$	$\|\Psi>=BD(2)-BD^{*}(1)=1.04*0.038$	1.72
$C48-O50^{\sigma}_{1.99177}$	$0.5573\,SP^{2.66}+0.8303\,SP^{2.42}$	$\|\Psi>=BD(1)-BD^{*}(1)=1.66*0.045$	1.48
$O50-C51^{\sigma}_{1.99230}$	$0.8331\,SP^{2.50}+0.5531\,SP^{3.90}$	$\|\Psi>=BD(1)-BD^{*}(1)=1.59*0.067$	3.41
$C51-H103^{\sigma}_{1.99195}$	$0.7822\,SP^{2.87}+0.6231\,S$	$\|\Psi>=BD(1)-BD^{*}(1)=1.230.063$	3.85
$C51-H104^{\sigma}_{1.99611}$	$0.7845\,SP^{2.73}+0.6202\,S$	$\|\Psi>=BD(1)-RY^{*}(1)=2.21*0.037$	0.76
$C51-H105^{\sigma}_{1.99599}$	$0.7852\,SP^{2.71}+0.6192\,S$	$\|\Psi>=BD(1)-RY^{*}(1)=2.210.038$	0.81

Table 7. Continued

$Bond^{BD}_{No.\ ele}$	Coefficients hybrids	$E_{acceptor(j)}$-$E_{Doner(i)*}$ Fack Matrix ($F_{i,j}$, a.u.)	E^2 (Kcal/mol)
$O52 - H106^{\sigma}_{1.98704}$	$0.8889\ SP^{2.68} + 0.4580\ S$	$\|\Psi> = BD\ (1) - BD^{*}\ (1) = 1.50*0.070$	4.02
$O53 - C54^{\sigma}_{1.99142}$	$0.8336\ SP^{2.44} + 0.5523\ SP^{2.66}$	$\|\Psi> = BD\ (1) - BD^{*}\ (1) = 1.69*0.046$	1.53
$C54 - O55^{\sigma}_{1.99667}$	$0.5798\ SP^{1.95} + 0.8147\ SP^{1.41}$	$\|\Psi> = BD\ (1) - BD^{*}\ (1) = 2.01*0.041$	1.05
$C54 - O55^{\pi}_{1.99190}$	$0.5247\ SP + 0.8513\ SP$	$\|\Psi> = BD\ (2) - BD^{*}\ (2) = 0.72*0.023$	0.88
		$\|\Psi> = BD\ (2) - BD^{*}\ (1) = 1.23*0.037$	1.41
$C54 - C56^{\sigma}_{1.98515}$	$0.7085\ SP^{1.57} + 0.7057\ SP^{3.01}$	$\|\Psi> = BD\ (1) - BD^{*}\ (1) = 1.34*0.069$	4.43
$C56 - H107^{\sigma}_{1.98096}$	$0.7927\ SP^{3.03} + 0.6096\ S$	$\|\Psi> = BD\ (1) - BD^{*}\ (1) = 1.53*0.058$	2.75
		$\|\Psi> = BD\ (1) - BD^{*}\ (2) = 0.86*0.067$	6.19
$C56 - H108^{\sigma}_{1.98923}$	$0.7923\ SP^{2.99} + 0.6102\ S$	$\|\Psi> = BD\ (1) - BD^{*}\ (1) = 1.23*0.074$	5.39
$C56 - H109^{\sigma}_{1.98097}$	$0.7970\ SP^{2.97} + 0.6040\ S$	$\|\Psi> = BD\ (1) - BD^{*}\ (1) = 0.86*0.067$	6.13
$C57 - C58^{\sigma}_{1.98686}$	$0.7072\ SP^{2.98} + 0.7070\ SP^{2.74}$	$\|\Psi> = BD\ (1) - BD^{*}\ (1) = 1.35*0.055$	2.81
$C57 - H110^{\sigma}_{1.98699}$	$0.7922\ SP^{3.00} + 0.6103\ S$	$\|\Psi> = BD\ (1) - BD^{*}\ (1) = 1.26*0.048$	2.26
$C57 - H111^{\sigma}_{1.98572}$	$0.7886\ SP^{3.15} + 0.6149\ S$	$\|\Psi> = BD\ (1) - BD^{*}\ (1) = 1.24*0.059$	3.51
$C58 - H112^{\sigma}_{1.99064}$	$0.7828\ SP^{2.92} + 0.6222\ S$	$\|\Psi> = BD\ (1) - BD^{*}\ (1) = 1.42*0.034$	1.05
$C58 - H113^{\sigma}_{1.98796}$	$0.7902\ SP^{2.90} + 0.6128\ S$	$\|\Psi> = BD\ (1) - BD^{*}\ (1) = 1.230.055$	3.11
$C59 - C60^{\sigma}_{1.99796}$	$0.8336\ SP^{2.54} + 0.5524\ SP^{3.88}$	$\|\Psi> = BD\ (1) - BD^{*}\ (1) = 1.89*0.070$	3.25
$C60 - H114^{\sigma}_{1.99572}$	$0.7823\ SP^{2.47} + 0.6229\ S$	$\|\Psi> = BD\ (1) - BD^{*}\ (1) = 1.26*0.024$	0.59
$C60 - H115^{\sigma}_{1.99082}$	$0.7871\ SP^{2.85} + 0.6169\ S$	$\|\Psi> = BD\ (1) - BD^{*}\ (1) = 1.26*0.065$	4.21
$C60 - H116^{\sigma}$	$0.7831\ SP^{2.73} + 0.6219\ S$	$\|\Psi> = BD\ (1) - BD^{*}\ (1) = 1.43*0.025$	0.53

calization' corrections to the zeroth-order natural Lewis structure. For each donor NBO (i) and acceptor NBO (j), the stabilization energy E (2) associated with delocalization ("2e-stabilization") is evaluated.

The strongest interaction at Hf/6-31G(d) level of calculation is appeared for the interaction of BD (1) C_5-H_9→ BD^* (1) C_8-C_{10} with E_2 = 9.39 Kcal/mol and BD (2) C_{30}-C_{31}→ BD^* (2) C_{29}-C_{32} with E_2 = 47.70 Kcal/mol for this compound. NBO analysis data have been also obtained by HF/3-21G(d), B3LYP/3-21G(d) and B3LYP/6-31G(d) levels of theory. The results can be found as a supplementary file. The strongest interaction at Hf/3-21G(d) level of calculation is identified for the interaction of BD(1) C_{29}-H_{32}→BD^* (1) C_{31}-C_{32} with E_2 = 8.43 Kcal/mol and BD (2) C_{30}-C_{31}→BD^* (2) C_{29}-C_{32} with E_2 = 47.62 Kcal/mol for this compound. The strongest interaction at B3LYP/6-31G(d) level of calculation is evaluated for the interaction of BD (1) C_5-H_9→BD^* (1) C_8-C_{10} with E_2 = 7.85 Kcal/mol and BD (2) C_{30}-C_{31}→BD^* (2) C_{29}-C_{32} with E_2 = 32.12 Kcal/mol for the titled compound. The strongest interaction in this compound at B3LYP/3-21G(d) level of calculation is identified for the interaction of BD (1) C_5-H_9→BD^* (1) C_8-C_{10} with E_2 = 6.95 Kcal/mol and BD (2) C_{30}-C_{31}→BD^* (2) C_{29}-C_{32} with E_2 = 23.01 Kcal/mol.

5. Conclusions

Nuclear magnetic resonance spectroscopy is a valuable technique for obtaining chemical information. Chemical shift anisotropy asymmetry (η), isotropy (σ_{iso}), anisotropy (σ_{aniso}), Δσ, K and chemical shift tensor (δ) were calculated based on theoretical data obtained from BL3Y/6-31G(d) and HF/6-31G(d). Moreover NBO analysis was performed and then stabilization energies, electron occupation at each bond and hybridation character around each atom were evaluated. We can say that intermolecular interaction effects such as electron transfer interactions play an important role in determining NMR chemical shielding tensors of the atoms. Comparison of experimental and computed data suggests the results obtained from HF/3-21g method are more acceptable. Moreover, E_{HOMO}, E_{LUMO} and E_{bg} were evaluated. The maximum and minimum values of E_{bg} were found in HF/3-21g and B3LYP/3-21g respectively. It was also found that O_{24}, O_{37}, O_{49} and O_{55} have minimum values of σ_{iso}, so these parts of the vincristine molecule may be considered as active sites for binding to tubulin or microtubule leading to its anticancer effects in process of cell division.

Acknowledgments

This work was supported by the Science and Research Branch, Islamic Azad University, Tehran, IR of Iran.

References

Borman, L.S. and Kuehne, M.E. 1989. Specific alterations in the biological activities of C- 20'- modified vinblastine congeners. Biochemical Pharmacology. 38, 715.

Borman, L.S. and Kuehne, M.E. 1990. Functionalhot spot at the C-20' position of vinblastine. In The Alkaloids, Antitumor bisindole alkaloids from catharanthus roseus (L.), A. Brossi and M. Suffness, editors. Volume 37. Academic Press. Inc., San Diego, California, U.S.A., pp. 133.

Damen, C. .N., Rosing, H., Schellens, J.H.M. and Beijnen, J. H. 2010. High-performance liquid chromatography coupled with mass spectrometry for the quantitative analysis of vinca-alkaloids in biological matrices: a concise survey from the literature. Biomedical Chromatography. 24, 83-90.

Dong, J.G., Bornmann, Nakanishi, W.K. and Berova, N. 1995. Structural studies of vinblastine alkaloids by exciton coupled circular dichroism. Phytochemistry. 40, 1821-1824.

Dowing, K.H. and Nogals, E. 1998. Tubulin and microtubule structure. Current Opinion in Cell Biology. 10, 16-22.

Dubrovay, Z., Hada, V., Beni, Z. and Szantay, C.Jr. 2013. NMR and mass spectrometric characterization of vinblastine, vincristine and some new related impurities – Part I. Journal of Pharmaceutical and Biomedical Analysis. 84, 293-308.

Gan, P.P. and Kavallaris, M. 2008. Tubulin-targeted drug action: functional significance of class ii and class IVb beta-tubulin in vinca alkaloid sensitivity. Cancer Research. 68, 9817-24.

Ghiasi, R. and Ebrahimi Mokaram, E., 2012. Natural Bond Orbital (NBO) Population Analysis of Iridabenzene $(C_5H_5Ir)(PH_3)_3$. Journal of Applied Chemical Research. 20, 7-13.

Himes, R.H. 1991. Interactions of the catharanthus (Vinca) alkaloids with tubulin and microtubules. Pharmacology and Therapeutics. 51, 257-267.

Johnson, I.S., 1968. Historical background of vinca alkaloid research and areas of future interest. Cancer Chemotherapy Reports. 52, 455–461.

Johnson, I.S., Wright, H.F. and Svoboda, G.H. 1959. Experimental basis for clinical evaluation of anti- tumor principles from Vinca rosea Linn. Journal of Laboratory and Clinical Medicine. 54, 830

Jordan, M.A. and Leslie, W. 2004. Microtubules as a target for anticancer drugs. Nature Reviews Cancer. 4, 253-265.

Kavallaris, M., Annereau, J.P. and Barret, J.M. 2008. Potential mechanisms of resistance to microtubule inhibitors. Seminars in Oncology. 35, 22-27.

Kosjek, T., Dolinšek, T., Gramec, D., Heath, E., Strojan. P., Serša, G. and Èemažar, M. 2013. Determination of vinblastine in tumour tissue with liquid chromatography-high resolution mass spectrometry. Talanta. 116, 887-893.

Kuehne, M.E. and Marko, I. 1990. Synthesis of vinblastine, type alkaloids. In The Alkaloids, A. Brossi and M. Suffness, editors. Volume 37. Academic Press. Inc., San Diego, California, U.S.A., pp. 133.

Lobert, S., Ingram, J.W. and Correia, J.J. 2007. The Thermodynamics of Vinca Alkaloid-Induced Tubulin Spiral Formation. Journal of Biophysical Chemistry. 126, 50-58.

March, N.H., Knapp- Mohammady, M., 2011. The Inhomogeneous Electron Liquid In Some Bioinorganic Assemblies Studied By Density Functional Methods. Physical Chemistry Liquid. 49, 259-269.

Martin-Galiano, A.J., Oliva, M.A., Sanz, L., Bhattacharyya, A., Serna, M., Yebenes, H., Valpuesta, J.M. and Andreu, J.M., 2011. Bacterial Tubulin Distinct Loop Sequences and Primitive Assembly Properties Support Its Origin from a Eukaryotic Tubulin Ancestor. Biological Chemistry. 286, 19789-19803.

Mollaamin, F., Najafpour, J., Ghadami, S., Ilkhani, A.R., Akrami, M.S. and Monajjemi, M. 2014a. The Electromagnetic Feature of $B_{15}N_{15}H_x$ (x = 0, 4, 8, 12, 16, and 20) Nano Rings: Quantum Theory of Atoms in Molecules/ NMR Approach. Journal of Computational and Theoretical Nanoscience. 11, 1290-1298.

Mollaamin, F., Monajjemi, M. and Mehrzad, J.V. 2014b. Molecular Modeling Investigation of an Anti-cancer Agent Joint to SWCNT Using Theoretical Methods. Fullerenes, Nanotubes and Carbon Nanostructures. 22, 738-751.

Monajjemi, M., Aghaie, H., Ardalan, P. and Mollaamin, F. 2011a. Investigation of nuclear magnetic resonance (NMR) shielding tensors of B5N5C8H18 cluster as a novel material for nano drug delivery. International Journal of Physical Sciences. 6, 7490-7504.

Monajjemi, M., Ahmadianarog, M., Mohmodi Hashemi, M. and Mollaamin, F. 2011b. NMR and natural bond orbital (NBO) calculation of glyoxals: Nano physical parameter investigation. International Journal of Physical Sciences. 6, 8063-8078.

Monajjemi, M. and Boggs, J.E. 2013. A new generation of B_nN_n rings as a supplement to boron nitride tubes and cages. The Journal of Physical Chemistry A. 117, 1670-1684.

Monajjemi, M., Kharghanian, L., Khaleghian, M. and Chegini, H. 2014a. Quantum Study of Amino Acid Bind to Carbon Nanotube in View of Magnetic Properties. Journal of Computational and Theoretical Nanoscience. 22, 709-725.

Monajjemi, M., Mollaamin, F. and Karimkeshteh, T. 2005. Ab initio study and hydrogen bonding calculations of nitrogen and carbon chemical shifts in serine-water complexes. Journal of the Mexican Chemical Society. 49, 344-352.

Monajjemi, M., Saedi, L., Najafi, F. and Mollaamin, F. 2010. Physical properties of active site of tubulin–binding as anticancer nanotechnology investigation. International Journal of Physical Sciences. 5, 1609-1621.

Monajjemi, M., Sobhanmanesh, A. and Mollaamin, F. 2011. Investigation of drug delivery on anticancer drug by SWCNT with theoretical studies. International Journal of Physical Sciences. 6, 6469-6478.

Monajjemi, M., Wayner, Jr. R. and Boggs, J.E. 2014b. NMR contour maps as a new parameter of carboxyl's OH groups in amino acids recognition: A reason of tRNA–amino acid conjugation. Chemical Physics. 433, 1-11.

Mordan, A. 2002. Mechanism of Action of Antitumor Drugs that Interact with Microtubules and Tubulin. Journal of Current Medicinal Chemistry: Anti-Cancer Agents. 2, 1-17.

Mousavi, M., Ilkhani, A.R., Sharifi, Sh., Mehrzad, J., Eghdami, A. and Monajjemi, M. 2013. DFT studies of nano anticancer on vinblastine and vincristine molecules. International Journal of Microbiology Research and Reviews. 1, 32-38.

Nafisi, S., Malekabady, Z.M., Khalilzadeh, M.A., 2010. Interaction of B-Carboline Alkaloids With RNA. DNA and Cell Biology. 29, 753–761.

Noble, R.L., Beer, C.T. and Cutts, J.H. 1958. Further biological activities of vincaleukoblastine- an alkaloid isolated from vinca rosea. Biochemical Pharmacology. 1, 347-348.

Sefzic, T.H., Turco, D., Iuliucci, R.J. and Facelli, J.C. 2005. Modeling NMR chemical shift: A survey of density functional theory approaches for calculating tensor properties. The Journal of Physical Chemistry A. 109, 1180-1187.